Far-from-equilibrium universality in the two-dimensional Heisenberg model

Joaquin F. Rodriguez-Nieva[a,1] , Asier Piñeiro Orioli[b], and Jamir Marino[c]

We characterize the universal far-from-equilibrium dynamics of the two-dimensional quantum Heisenberg magnet isolated from its environment. For a broad range of initial conditions, we find a long-lived universal prethermal regime characterized by self-similar behavior of spin–spin correlations. We analytically derive the spatial–temporal scaling exponents and find excellent agreement with numerics using phase space methods. The scaling exponents are insensitive to the choice of initial conditions, which include coherent and incoherent spin states with values of total magnetization and energy in a wide range. Compared to previously studied self-similar dynamics in nonequilibrium $O(n)$ field theories and Bose gases, we find qualitatively distinct scaling behavior originating from the presence of spin modes that remain gapless at long times and are protected by the global SU(2) symmetry. Our predictions, which suggest a distinct nonequilibrium universality class from Bose gases and $O(n)$ theories, are readily testable in ultracold atoms simulators of Heisenberg magnets.

universality | spin dynamics | self-similarity | nonequilibrium

Extending the paradigm of universality to far-from-equilibrium regimes is a current frontier in physics. A distinguishing feature of universal dynamics in complex systems is the emergence of self-similar behavior. Close to equilibrium, diverse and seemingly distinct models can be classified using symmetry and dimensionality into universality classes sharing the same self-similar scaling (1). Far from equilibrium, however, the system can break a symmetry concomitant with detailed balance (2, 3) and can therefore exhibit self-similar dynamics beyond conventional equilibrium paradigms. Celebrated examples include turbulence (4, 5), aging (6), phase-ordering kinetics (7–9), Kardar-Parisi-Zhang (KPZ) scaling (10), reaction–diffusion models, and percolation (11).

Universality and self-similar relaxation typically arise in open systems with external friction and noisy forces that drive the system to or across a critical point (1, 11–15). Remarkably, recent theoretical works have shown that self-similar scaling can also occur in isolated systems where the system acts as its own bath. Prominent examples of dynamical scaling in isolated quantum many-body systems include prethermal critical states (6, 16–27) and nonthermal fixed points in scalar and gauge theories (28–44). Research into these phenomena is further fueled by a surge of experimental evidence for universal dynamics in cold atoms (45–51) and dynamical phase transitions in trapped ions (52) and cavity quantum electrodynamics (53).

Despite the ubiquity of spin models in condensed-matter and cold atom experiments, a systematic classification of nonequilibrium universality in such systems is still lacking. Indeed, nonequilibrium universality has mostly been explored analytically and numerically in models with $U(n)$ and $O(n)$ symmetries where self-similarity arises in the regime of large bosonic occupations (33–35, 39, 54, 55) or for quantum quenches in the $n \to \infty$ limit (16, 18, 19, 22, 24). Recent experiments in cold atomic gases have started to probe these nonequilibrium bosonic regimes (45–50) and have also paved the way to explore other dynamical regimes in fully tunable spin systems (56–58), including tunable symmetries and the spatial dimension. Relevant to this generation of experiments, here we show that the two-dimensional isotropic Heisenberg model at finite energy exhibits a nonthermal fixed point that is qualitatively distinct from previous instances of scaling, and we characterize its universal properties analytically and numerically.

Central to our discussion is the role of dimensionality $d = 2$ and the presence of global SU(2) symmetry. First, the absence of a finite-temperature symmetry-breaking phase transition in $d = 2$ precludes scaling due to other well-studied phenomena like coarsening or aging. Having two dimensions also bestows on magnetization fluctuations a quasi–long-range character, which is an essential feature used to analytically compute the scaling exponents. Second, the global SU(2) symmetry constrains the nature of excitations in the system and their corresponding interactions. For instance, a recent work by one of us (59) showed that, close to the fully polarized ferromagnetic ground state, the SU(2) symmetry

Significance

Universal scaling in far-from-equilibrium regimes typically emerges in systems quenched across a finite-temperature phase transition or close to nonthermal fixed points of bosonic systems. Such dynamical regimes have been extensively studied in the context of interacting Bose gases and O(n) field theories. Recent experiments in cold atomic gases have opened additional pathways to explore the dynamics of quantum magnets with exquisite control of symmetries and dimensionality. Relevant to this generation of experiments, we introduce a different paradigm for nonequilibrium scaling in spin systems quenched at the critical dimension $d_c = 2$ wherein symmetry-protected, gapless modes with long-range character dominate the spatial–temporal scaling. This yields a nonequilibrium universality class qualitatively distinct from previously studied U(1) and O(n) theories.

[1]To whom correspondence may be addressed. Email: jrodrieznieva@stanford.edu.
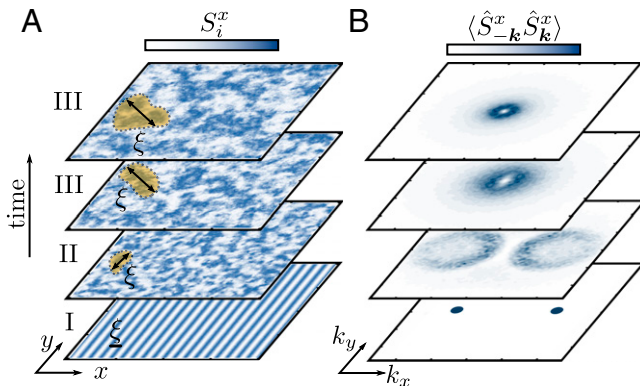
constrains the interaction between magnons (the low-energy bosonic-like quasiparticles) and gives rise to slow magnon relaxation with anomalous scaling (59). Here we show that the combination of symmetry and dimensionality alone, without any further assumptions like proximity to the fully polarized ground state or bosonic approximations, can lead to a universal prethermal regime that is dominated by gapless spin modes and is qualitatively distinct from previously studied U(n) and O(n) theories in several important ways, as we discuss below.

More specifically, starting from an initial textured state with a characteristic wavevector q, we show that the equal-time spin–spin correlation functions exhibit self-similar scaling in a wide intermediate-time window,

$$\sum_{a=x,y,z} \langle \hat{S}^a_{-\boldsymbol{k}}(t) \hat{S}^a_{\boldsymbol{k}}(t) \rangle = t^\alpha \Phi(t^\beta |\boldsymbol{k}|), \qquad \text{[1]}$$

for a broad range of initial conditions and arbitrary spin number S. The spatial–temporal scaling exponents (α, β) are independent of the details of the initial conditions, whereas the universal function Φ is only sensitive to a combination of q and the global magnetization of the initial state. In a loose sense, the initial length scale of the spin texture $\xi = 1/q$ defines a dynamical renormalization group integration scale that governs the temporal scaling of correlation functions (Fig. 1). Using this physical picture, combined with analytical considerations based on symmetries and the structure of the equations of motion, we derive analytically the scaling exponents for a Gaussian and an interacting nonthermal fixed point and find excellent agreement with numerics using the truncated Wigner approximation (TWA) (60, 61). We also observe numerically the dynamical cross-over from the Gaussian to the interacting nonthermal fixed point. Remarkably, our results, $\alpha = \beta d$ and $\beta = 1/3$, agree within numerical uncertainties with the exponents found for magnon dynamics close to the ferromagnetic state (59), therefore suggesting the existence of a single nonthermal fixed point encompassing very broad energy and magnetization sectors. This contrasts with bosonic theories where different initial conditions can lead to different scaling regimes (30). The present results, combined with those in a recent work by one of us (62) that found the asymptotic behavior $\Phi(x) \sim x^{-\nu_E}$ (with $\nu_E = 10/3$) using wave turbulence theory, allow us to fully characterize the universal spatial–temporal features of the nonthermal fixed point in terms of the three universal numbers α, β, and ν_E.

A key insight of the present work is that the intermediate-time self-similar dynamics are governed by gapless spin excitations whose gapless nature is protected by the global SU(2) symmetry. We demonstrate this numerically by computing unequal-time correlations (54, 55, 63–65), where we find that the effective gap, or energy ω_k required to excite a long-wavelength mode on top of the prethermal state, remains zero at long times irrespective of the initial conditions or model parameters, as long as SU(2) is preserved. This circumstance is a hallmark of our model. In contrast, the effective gap to excite quasiparticles in O(n) models out of equilibrium is not protected and typically grows due to the interplay between fluctuations and quartic interactions (16, 18, 21, 24, 33, 54, 55). When SU(2) is reduced to U(1) in our model, we find different scaling exponents, therefore reinforcing the distinction between nonequilibrium universality in the isotropic Heisenberg model and previous instances of scaling in U(1) models.

In the spirit of the Halperin–Hohenberg classification (1), the values of (α, β) that we find, combined with the presence of an additional slow mode with quadratic dispersion, suggest that the Heisenberg model belongs to a different nonequilibrium universality class than Bose gases (33–36, 39, 54, 55), dissipative $O(n)$ models (66–70), and other nonintegrable high-dimensional spin systems (59, 62, 71–78), as we discuss below. This is quite surprising in light of the well-known similarities between the Heisenberg model and O(3) scalar models at equilibrium. We emphasize, however, that the scaling regime discussed in the present work is intrinsically different from the predictions of the Halperin–Hohenberg classification: While the latter describes universal behavior close to thermodynamic equilibrium, here we consider a dynamical regime where equilibrium properties, such as the fluctuation–dissipation relation, are violated.

Microscopic Model

We consider the two-dimensional isotropic Heisenberg model on a square $L \times L$ lattice with lattice constant ℓ and total number of sites $N = L^2$:

$$\hat{H} = -J \sum_{\langle i,j \rangle} \left(\hat{S}^x_i \hat{S}^x_j + \hat{S}^y_i \hat{S}^y_j + \hat{S}^z_i \hat{S}^z_j \right), \qquad \text{[2]}$$

where $\langle i, j \rangle$ denotes summation over nearest neighbors. Each site has a spin S degree of freedom and periodic boundary conditions are used in each spatial direction. This model has an SU(2) symmetry with conserved global spin magnetization $S^a \equiv \sum_i \langle \hat{S}^a_i \rangle$ for $a \in \{x, y, z\}$, where $\langle \cdot \rangle$ denotes the quantum expectation value.

As an initial condition, we consider an uncorrelated pure product state where the spins form a spiral in real space parameterized by a wavevector $\boldsymbol{q}$ and angle θ,

$$\langle \hat{S}^\pm_i(0) \rangle = S \sin\theta \, e^{\pm i \boldsymbol{q} \cdot \boldsymbol{r}_i}, \quad \langle \hat{S}^z_i(0) \rangle = S \cos\theta, \qquad \text{[3]}$$

with $\hat{S}^\pm_i = \hat{S}^x_i \pm i \hat{S}^y_i$ and $\boldsymbol{r}_i$ the position of site i. Other classes of initial conditions are considered in *SI Appendix*. Eq. **3** defines a characteristic timescale $1/\tau_* = JS^2 \sin^2\theta [2 - \cos(q_x \ell) - \cos(q_y \ell)]$ associated to the energy density of the initial state.

Spatial–Temporal Scaling via Phase Space Methods

We begin by computing the real-time dynamics using TWA (79). This method incorporates quantum fluctuations present in the initial state by considering classical spins $\boldsymbol{S}_i = (S^x_i, S^y_i, S^z_i)$ with

Fig. 1. Evolution of the spin–spin correlation function starting from an initially uncorrelated spin spiral state along the $\hat{x}$ direction for the two-dimensional Heisenberg model. The stages of relaxation are I) instability triggered by quantum fluctuations, II) depletion of the macroscopically occupied state, and III) growth of magnetization fluctuations with a time-dependent correlation length ξ (shown at two different times). *A* shows a single semiclassical realization of spin S^x_i configurations in real space, and *B* shows the (quantum) spin–spin correlation function in momentum space.

quantum noise at $t = 0$ and evolving them with the classical Landau–Lifshitz equations of motion. Defining $\boldsymbol{S}_i^\perp$ as the transverse magnetization to $\langle \hat{\boldsymbol{S}}_i(0) \rangle$ for the initial condition **3**, we assume initial Gaussian fluctuations of $\boldsymbol{S}_i^\perp$ given by $\langle \boldsymbol{S}_i^\perp \rangle_{\rm cl} = 0$ and $\langle \boldsymbol{S}_i^\perp \cdot \boldsymbol{S}_i^\perp \rangle_{\rm cl} = S$, where $\langle \cdot \rangle_{\rm cl}$ denotes the average over classical trajectories.

The subsequent dynamics follow three relaxation stages as illustrated in Fig. 1: I) Quantum fluctuations trigger a dynamical instability that leads to II) a depletion of the macroscopically occupied state **q** and is followed by III) a scaling regime in which magnetization fluctuations grow with a time-dependent correlation length $\xi(t) \sim t^\beta$, which exhibits self-similar evolution following Eq. **1**.

Fig. 2A shows the evolution of the spin–spin correlation function $\sum_a \langle \hat{S}_{-\boldsymbol{k}}^a(t) \hat{S}_{\boldsymbol{k}}^a(t) \rangle$ during the three stages of relaxation for a full spiral ($\theta = \pi/2$).* Here, $\hat{S}_{\boldsymbol{k}}^a = \frac{1}{\sqrt{N}} \sum_i e^{i\boldsymbol{k}\cdot\boldsymbol{r}_i} \hat{S}_i^a$ denotes the discrete Fourier transform with wavevector $\boldsymbol{k}$. The decay of the initial macroscopically occupied mode $\boldsymbol{q}$ (solid line) occurs on a timescale of approximately $4\tau_*$ (72) and leads to a quick redistribution of fluctuations into other $\boldsymbol{k}$ modes (stages I and II in Fig. 1; dotted lines in Fig. 2A). At later times (stage III in Fig. 1; blue dashed lines in Fig. 2A) the system exhibits self-similarity as
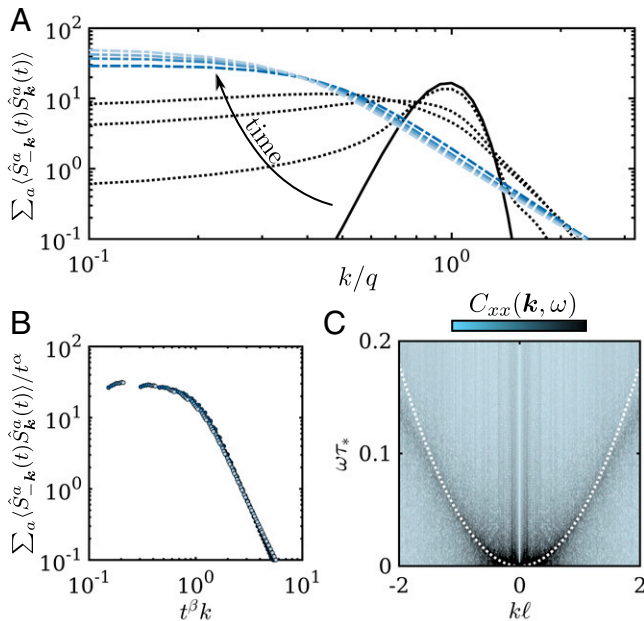
Fig. 2. (A) Evolution of the spin–spin correlation function $\sum_a \langle \hat{S}_{-\boldsymbol{k}}^a \hat{S}_{\boldsymbol{k}}^a \rangle$ after a quench from an initial spin spiral. Shown with solid and dotted lines are the initial distribution and the process of depletion of the initial q mode (stages I and II), respectively. We show with colored dashed lines the spin–spin correlation in the self-similar regime (stage III). Dotted lines are plotted for $t/\tau_* = 3, 4, 5$, and dashed lines are plotted for the range $15 < t/\tau_* < 40$, with lighter colors for increasing t. (B) Collapsed datapoints during stage III (Eq. **1**) with scaling exponents $\alpha = \frac{2}{3}$ and $\beta = \frac{1}{3}$. (C) Fourier transform of the unequal-time spin–spin correlation function $C_{xx}(\boldsymbol{k}, \omega) \equiv \int dt\, e^{i\omega t} \langle \frac{1}{2} \{ \hat{S}_{-\boldsymbol{k}}^x(t_0 + t), \hat{S}_{\boldsymbol{k}}^x(t_0) \} \rangle$ for $t_0 = 20\tau_*$. Different values of t_0 do not affect the qualitative features of the plot. Shown with dotted lines is a quadratic fit of the mode dispersion. Simulation parameters: $L = 800$, $q_x = 0.2$, $\theta = \pi/2$, $S = 5$.

---

*In TWA, correlation functions of classical variables correspond to quantum expectation values of symmetrized operators (79). In particular, we have $\langle \frac{1}{2} \{ \hat{S}_{-\boldsymbol{k}}^a(t), \hat{S}_{\boldsymbol{k}}^a(t') \} \rangle \approx \langle S_{-\boldsymbol{k}}^a(t) S_{\boldsymbol{k}}^a(t') \rangle_{\rm cl}$, where $\{ \hat{A}, \hat{B} \} \equiv \hat{A}\hat{B} + \hat{B}\hat{A}$. Note that for equal times, $\langle \frac{1}{2} \{ \hat{S}_{-\boldsymbol{k}}^a(t), \hat{S}_{\boldsymbol{k}}^a(t) \} \rangle = \langle \hat{S}_{-\boldsymbol{k}}^a(t), \hat{S}_{\boldsymbol{k}}^a(t) \rangle$.

demonstrated in Fig. 2B by the excellent collapse of the rescaled curves with

$$\alpha = 0.63 \pm 0.05, \quad \beta = 0.34 \pm 0.03, \qquad [4]$$

which also agree with our analytical estimates below (the procedure for fitting the exponents is discussed in *SI Appendix*).

The SU(2) symmetry of the Heisenberg model precludes the opening of an effective gap during the dynamics. To find the relevant excitations, we evaluate in Fig. 2C the unequal-time spin–spin correlation functions in frequency space, $C_{xx}(\boldsymbol{k}, \omega) \equiv \int dt\, e^{i\omega t} \langle \frac{1}{2} \{ \hat{S}_{-\boldsymbol{k}}^x(t_0 + t), \hat{S}_{\boldsymbol{k}}^x(t_0) \} \rangle$, for intermediate times t_0.* This shows that the self-similar dynamics are governed by gapless excitations at all timescales t_0, even when the initial state is far from the fully polarized ground state. The dispersion of this mode is consistent with $\omega \sim k^2$ (white dotted line in Fig. 2C) for wavevectors $k\ell \gtrsim 0.08$ below which finite-size effects become sizable.

Derivation of the Scaling Exponents (α, β)

We now analytically estimate the scaling exponents assuming for simplicity that the system has no net magnetization (nonzero magnetization does not affect the argument in any essential way). In this case, spin–spin fluctuations eventually become isotropic both in real and in spin space. We find this to occur after a short transient timescale $\approx 5\tau_*$ (Fig. 1 and *SI Appendix*) and, therefore, the three components of the spin–spin correlation function exhibit the same scaling. In addition, we find that the mean-field components $\langle \hat{S}_{\boldsymbol{k}}^a(t) \rangle$ vanish on average at the onset of stage III. As a result, we use the full and connected component of $\langle \hat{S}_{-\boldsymbol{k}}^a(t) \hat{S}_{\boldsymbol{k}}^a(t) \rangle$ indistinguishably.

The first relation between α and β is obtained from the local constraint of spin operators $\hat{\boldsymbol{S}}_i \cdot \hat{\boldsymbol{S}}_i = S(S+1)$. In momentum space, this relation is written as

$$\frac{1}{N} \sum_{\boldsymbol{k}, a} \hat{S}_{-\boldsymbol{k}}^a \hat{S}_{\boldsymbol{k}}^a = S(S+1). \qquad [5]$$

Eq. **5** is an exact relation that is independent of the state of the system. If the spin–spin correlation function satisfies Eq. **1**, then Eq. **5** implies that $t^{\alpha - d\beta} \int \frac{d^d\boldsymbol{x}}{(2\pi)^d} \Phi(|\boldsymbol{x}|)$ is a constant or, equivalently, that α and β are related through

$$\alpha = d\beta. \qquad [6]$$

Interestingly, we note that the relation **6** also appears in other scaling regimes of different microscopic nature. For instance, Eq. **6** appears in coarsening dynamics when one assumes that correlations are governed by a single length scale given by the typical size of the ordered regions (equation 7 in ref. 7). It also appears in the universal dynamics of a Bose gas (33), where Eq. **6** is equivalent to boson number conservation in the self-similar range. Here, instead, Eq. **6** is a consequence of the constraint on spin length.

The second relation between α and β is obtained from dynamics. The time dependence of the spin–spin correlation function $\langle \hat{S}_{-\boldsymbol{k}}^a \hat{S}_{\boldsymbol{k}}^a \rangle$ can be straightforwardly obtained from the microscopic equations of motion of the spin operators, $\partial_t \hat{S}_i^a = \sum_{j,b,c} \epsilon_{abc} \hat{S}_i^b \hat{S}_j^c$, which yields

$$\partial_t \langle \hat{S}_{-\boldsymbol{k}}^a \hat{S}_{\boldsymbol{k}}^a \rangle = 2 \sum_{\boldsymbol{p}, b, c} (\gamma_0 - \gamma_{\boldsymbol{p}}) \text{Re} \left[\epsilon_{abc} \langle \hat{S}_{-\boldsymbol{k}}^a \hat{S}_{\boldsymbol{k}-\boldsymbol{p}}^b \hat{S}_{\boldsymbol{p}}^c \rangle \right], \quad [7]$$

where $\gamma_{\boldsymbol{p}} = \sum_{\boldsymbol{\ell}} e^{i\boldsymbol{p}\cdot\boldsymbol{\ell}}$ ($\boldsymbol{\ell}$ are unit cell vectors) (details in *SI Appendix*). The central assumption in our derivation is that a single length scale ξ governs the scaling of two- and three-point correlation functions. The validity of such a stringent assumption can be justified from the long-range character of spin modes and the absence of other characteristic length scales in $d = 2$ (e.g., a nonzero effective gap or localized defects). This translates to modes being macroscopically and democratically occupied within a region $\boldsymbol{k} \lesssim 1/\xi$, contrary to a conventional condensate with long-range order where a single mode $\boldsymbol{k} = 0$ is macroscopically occupied. Such quasi–long-range character in a low-dimensional system is often referred to as a quasi-condensate (80). In addition, the rate of change of ξ is assumed to be much slower than the microscopic timescale τ_* defined above, such that fast microscopic fluctuations can be integrated out. As a result, dimensional analysis of Eq. **1** suggests that $\mathrm{Re}\left[\epsilon_{abc}\langle \hat{S}_{-\boldsymbol{k}}^a \hat{S}_{\boldsymbol{k}-\boldsymbol{p}}^b \hat{S}_{\boldsymbol{p}}^c \rangle\right] \sim \xi^{3\alpha/2\beta}\Psi(\boldsymbol{k}\xi, \boldsymbol{p}\xi)$, with $\xi \sim t^\beta$ and Ψ a scaling function. Using this scaling form in the right-hand side of Eq. **7** in the long-wavelength limit [i.e., taking $\gamma_0 - \gamma_{\boldsymbol{q}} \approx (\boldsymbol{q}\ell)^2$] yields $\xi^{3\alpha/2\beta-d-2}\Psi'(\boldsymbol{k}\xi)$, with $\Psi'(\boldsymbol{x}) = \int \frac{d^d\boldsymbol{y}}{(2\pi)^d}\boldsymbol{y}^2\Psi(\boldsymbol{x}, \boldsymbol{y})$. In addition, the left-hand side of Eq. **7** scales as $\xi^{\alpha/\beta-1/\beta}$. Equating the scaling form on both sides of Eq. **7** results in

$$2(d+2)\beta = \alpha + 2. \qquad [8]$$

Combining Eqs. **8** and **6** in $d = 2$ yields $\alpha = \frac{2}{3}$ and $\beta = \frac{1}{3}$, consistent with the numerical results in Eq. **4** and with the scaling found numerically within kinetic theory close to the ferromagnetic ground state with $\theta \approx 0$ (59) (we note that kinetic theory failed to analytically yield the correct exponents from scaling arguments alone). We emphasize again that Eq. **8** is valid only in $d = 2$ as it relies on spin modes having a long-range character (in $d = 3$, for example, the initial spin texture will collapse into localized skyrmions giving rise to qualitatively different prethermal dynamics).

The Universal Scaling Function

So far, we considered the dynamics of a single dimensionless parameter ξ/ℓ that governs the self-similar scaling. In addition, we empirically find that the scaling function Φ in Eq. **1** is sensitive to the magnetization sector of the state through the dimensionless ratio

$$\Theta = \frac{\tan\theta}{q\ell}, \qquad [9]$$

as shown in Fig. 3. If $\theta = \pi/2$, then $\Theta \to \infty$ and the scaling function becomes independent of q. For other values of θ and q, we find an excellent collapse of the data points.

We note that the dimensionless parameter Θ essentially quantifies the ratio between magnetization fluctuations and the global magnetization, as we discuss next. The average magnetization is given by $S^z/N = S\cos\theta$. The average amplitude of magnetization fluctuations at the onset of stage III is obtained from the identity (5) after removing the disconnected component associated to the global magnetization, which scales as $S^2\cos^2\theta$, and assuming that fluctuations are equally distributed in a phase space region of size $|\boldsymbol{k}| \lesssim q$. For large S, this results in $\sum_a \langle S_{-\boldsymbol{k}}^a S_{\boldsymbol{k}}^a \rangle_c \sim (S\sin\theta q\ell)^2$, where "c" stands for connected. The ratio between these two quantities gives the empirical Eq. **9**.

Dynamical Crossovers

The self-similar scaling regime described above cannot be captured by an effective Gaussian description. This can be readily checked using a self-consistent Holstein–Primakoff approximation in the low spin-wave density expansion (73, 81), which would instead yield $\alpha = 1$ and $\beta = 1/2$ for the $d = 2$ Heisenberg model (*SI Appendix*). Interestingly, these Gaussian exponents can be observed at early times before crossing over into the nonthermal fixed point. An instance of this dynamical cross-over, which is reminiscent of the phenomenon of prescaling (82, 83), is reported in *SI Appendix*. Therefore, two dynamical cross-overs occur in the Heisenberg model: The first one accompanies dynamics from a Gaussian to a non-Gaussian fixed point, while the second one dictates the approach to the thermal state, which is the fate of dynamics for generic high-dimensional nonintegrable systems.

Discussion

The self-similar exponents and scaling functions obtained here are distinct from those found in previous works on nonequilibrium dynamics in classical and quantum O(n) field theories and U(n) bosonic models (33–36, 54, 55). Compared to these previous works, the central difference of our results is that the dynamics of the Heisenberg model are dominated by gapless spin excitations at all times. This is in sharp contrast to typical nonthermal fixed points in bosonic theories, where an effective gap has been observed to be dynamically generated by fluctuations (33, 54, 55). This effective gap has been shown to lead to a modified (nonrelativistic) effective theory at low momenta, which is characterized by different scaling exponents from those of the gapless theory. Our results also differ from scaling dynamics of O(n) theories quenched to (or across) a critical point (16, 18, 21, 24),
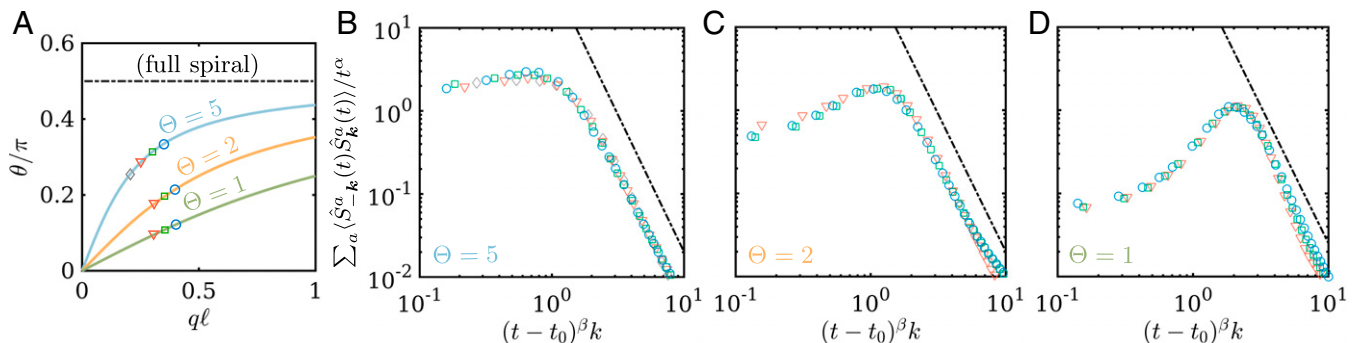
Fig. 3. Self-similar scaling of the spin–spin correlation functions shown for initial conditions with the same value of $\Theta = \tan\theta/(q\ell)$. In B–D, different symbols denote initial conditions with the different values of (q, θ) shown in A. When collapsing the datapoints, we allow for a finite time shift t_0 to account for the initial-condition–dependent dephasing time. Shown with dash-dotted lines is the universal power-law scaling $\sim k^{-10/3}$ associated to spin turbulence (62).

where a dynamically generated gap only vanishes asymptotically in time: In these works, self-similarity occurs only if parameters and initial conditions are fine-tuned to guarantee a vanishing late-time effective gap. Compared to these bosonic theories, the interaction vertex of the Heisenberg model is "soft" after a spin wave expansion (73, 81); i.e., it contains spatial gradients that are absent in O(n) models (*SI Appendix*). This already sets a difference at the level of canonical power counting and suggests that the two models cannot belong to the same universality class (*SI Appendix*).

To further demonstrate the importance of the SU(2) symmetry, we show in *SI Appendix* that, by adding anisotropic exchange $\hat{H} = \delta J_z \sum_{\langle i,j \rangle} \hat{S}_i^z \hat{S}_j^z$ to Eq. **2**, the dynamical exponents flow to a different nonthermal fixed point. In particular, for the easy-plane case ($\delta J_z > 0$) wherein the global symmetry is instead U(1), we obtain the same scaling exponents $\alpha = 1$, $\beta = 1/2$ as those observed in bosonic O(n) and U(n) theories (33–35, 39).

Conclusions

Our results on self-similar relaxation in the Heisenberg model extend to spin systems the paradigm of scaling in the proximity of nonthermal fixed points, which were so far thoroughly studied only for interacting bosonic and gauge theories (28–44). Cold atoms experiments have so far explored far-from-equilibrium transport and relaxation of one-dimensional quantum Heisenberg models (56, 57). We believe that our results provide strong motivation to extend quantum simulators of spin models to higher dimensionality, where integrability is less prominent in constraining quantum dynamics. Another natural next step toward implementations would consist in considering long-range spin interactions $\propto 1/r^\zeta$, with the perspective to investigate the dependence of dynamical scaling exponents with ζ (see ref. 84 for an equilibrium counterpart).

Our work opens up at least two interesting research avenues to explore. On the one hand, we have found scaling exponents that are remarkably robust to initial conditions belonging to different energy and magnetization sectors. It would be interesting to investigate whether this applies to other spin models with, e.g., SU(n) symmetric interactions, which can also be studied in cold atom experiments (85). On the other hand, our work has highlighted the essential role played by the symmetry-protected gaplessness of spin excitations. This poses the question of whether the scaling exponents observed in this work can also be reproduced in O(n) models under conditions that might have been overlooked so far or whether the Heisenberg spin model far from equilibrium is fundamentally different from O(n) models. The latter would clash with equilibrium common wisdom and reinforce the intuition that nonequilibrium scaling is governed by intrinsically different mechanisms than equilibrium universality.

Author affiliations: ªDepartment of Physics, Stanford University, Stanford, CA 94305; ᵇJILA, Department of Physics, University of Colorado Boulder, Boulder, CO 80309; and ᶜInstitut für Physik, Johannes Gutenberg Universität Mainz, D-55099 Mainz, Germany

1. P. C. Hohenberg, B. I. Halperin, Theory of dynamic critical phenomena. *Rev. Mod. Phys.* **49**, 435–479 (1977).
2. L. Sieberer, A. Chiocchetta, A. Gambassi, U. Täuber, S. Diehl, Thermodynamic equilibrium as a symmetry of the Schwinger-Keldysh action. *Phys. Rev. B Condens. Matter Mater. Phys.* **92**, 134307 (2015).
3. C. Aron, G. Biroli, L. Cugliandolo, (Non) equilibrium dynamics: A (broken) symmetry of the keldysh generating functional. *SciPost Phys.* **4**, 008 (2018).
4. U. Frisch, *Turbulence: The Legacy of A. N. Kolmogorov* (Cambridge University Press, 1995).
5. V. Zakharov, V. L'vov, G. Falkovich, *Kolmogorov Spectra of Turbulence* (Springer-Verlag, 1992), .
6. P. Calabrese, A. Gambassi, Ageing properties of critical systems. *J. Phys. Math. Gen.* **38**, R133 (2005).
7. A. Bray, Theory of phase-ordering kinetics. *Adv. Phys.* **43**, 357–459 (1994).
8. G. Biroli, L. F. Cugliandolo, A. Sicilia, Kibble-Zurek mechanism and infinitely slow annealing through critical points. *Phys. Rev. E Stat. Nonlin. Soft Matter Phys.* **81**, 050101 (2010).
9. A. Jelić, L. F. Cugliandolo, Quench dynamics of the 2d xy model. *J. Stat. Mech. Theory Exp.* **2011**, P02032 (2011).
10. M. Kardar, G. Parisi, Y. C. Zhang, Dynamic scaling of growing interfaces. *Phys. Rev. Lett.* **56**, 889–892 (1986).
11. U. C. Täuber, *Critical Dynamics: A Field Theory Approach to Equilibrium and Non-Equilibrium Scaling Behavior* (Cambridge University Press, 2014).
12. L. M. Sieberer, S. D. Huber, E. Altman, S. Diehl, Dynamical critical phenomena in driven-dissipative systems. *Phys. Rev. Lett.* **110**, 195301 (2013).
13. E. G. Dalla Torre, E. Demler, T. Giamarchi, E. Altman, Dynamics and universality in noise-driven dissipative systems. *Phys. Rev. B Condens. Matter Mater. Phys.* **85**, 184302 (2012).
14. J. Marino, S. Diehl, Quantum dynamical field theory for nonequilibrium phase transitions in driven open systems. *Phys. Rev. B* **94**, 085150 (2016).
15. A. Mitra, S. Takei, Y. B. Kim, A. J. Millis, Nonequilibrium quantum criticality in open electronic systems. *Phys. Rev. Lett.* **97**, 236808 (2006).
16. A. Chandran, A. Nanduri, S. S. Gubser, S. L. Sondhi, Equilibration and coarsening in the quantum O(N) model at infinite N. *Phys. Rev. B Condens. Matter Mater. Phys.* **88**, 024306 (2013).
17. P. Gagel, P. P. Orth, J. Schmalian, Universal postquench coarsening and aging at a quantum critical point. *Phys. Rev. B Condens. Matter Mater. Phys.* **92**, 115121 (2015).
18. A. Maraga, A. Chiocchetta, A. Mitra, A. Gambassi, Aging and coarsening in isolated quantum systems after a quench: Exact results for the quantum O(N) model with $N \to \infty$. *Phys. Rev. E Stat. Nonlin. Soft Matter Phys.* **92**, 042151 (2015).
19. A. Gambassi, P. Calabrese, Quantum quenches as classical critical films. *Europhys. Lett.* **95**, 66007 (2011).
20. B. Sciolla, G. Biroli, Quantum quenches, dynamical transitions, and off-equilibrium quantum criticality. *Phys. Rev. B Condens. Matter Mater. Phys.* **88**, 201110 (2013).
21. P. Smacchia, M. Knap, E. Demler, A. Silva, Exploring dynamical phase transitions and prethermalization with quantum noise of excitations. *Phys. Rev. B Condens. Matter Mater. Phys.* **91**, 205136 (2015).
22. P. Gagel, P. P. Orth, J. Schmalian, Universal postquench prethermalization at a quantum critical point. *Phys. Rev. Lett.* **113**, 220401 (2014).
23. A. Chiocchetta, M. Tavora, A. Gambassi, A. Mitra, Short-time universal scaling and light-cone dynamics after a quench in an isolated quantum system in d spatial dimensions. *Phys. Rev. B* **94**, 134311 (2016).
24. A. Chiocchetta, A. Gambassi, S. Diehl, J. Marino, Dynamical crossovers in prethermal critical states. *Phys. Rev. Lett.* **118**, 135701 (2017).
25. A. Chiocchetta, A. Gambassi, S. Diehl, J. Marino, Universal short-time dynamics: Boundary functional renormalization group for a temperature quench. *Phys. Rev. B* **94**, 174301 (2016).
26. A. Lerose, B. Žunkovič, J. Marino, A. Gambassi, A. Silva, Impact of nonequilibrium fluctuations on prethermal dynamical phase transitions in long-range interacting spin chains. *Phys. Rev. B* **99**, 045128 (2019).
27. A. Lerose, J. Marino, B. Žunkovič, A. Gambassi, A. Silva, Chaotic dynamical ferromagnetic phase induced by nonequilibrium quantum fluctuations. *Phys. Rev. Lett.* **120**, 130603 (2018).
28. J. Berges, A. Rothkopf, J. Schmidt, Nonthermal fixed points: Effective weak coupling for strongly correlated systems far from equilibrium. *Phys. Rev. Lett.* **101**, 041603 (2008).
29. R. Micha, I. I. Tkachev, Turbulent thermalization. *Phys. Rev. D Part. Fields Gravit. Cosmol.* **70**, 043538 (2004).
30. B. Nowak, D. Sexty, T. Gasenzer, Superfluid turbulence: Nonthermal fixed point in an ultracold Bose gas. *Phys. Rev. B Condens. Matter Mater. Phys.* **84**, 020506 (2011).
31. J. Berges, D. Sexty, Bose condensation far from equilibrium. *Phys. Rev. Lett.* **108**, 161601 (2012).
32. B. Nowak, J. Schole, D. Sexty, T. Gasenzer, Nonthermal fixed points, vortex statistics, and superfluid turbulence in an ultracold Bose gas. *Phys. Rev. A* **85**, 043627 (2012).
33. A. Piñeiro Orioli, K. Boguslavski, J. Berges, Universal self-similar dynamics of relativistic and nonrelativistic field theories near nonthermal fixed points. *Phys. Rev. D Part. Fields Gravit. Cosmol.* **92**, 025041 (2015).
34. M. Karl, T. Gasenzer, Strongly anomalous non-thermal fixed point in a quenched two-dimensional Bose gas. *New J. Phys.* **19**, 093014 (2017).
35. A. N. Mikheev, C. M. Schmied, T. Gasenzer, Low-energy effective theory of nonthermal fixed points in a multicomponent Bose gas. *Phys. Rev. A (Coll. Park)* **99**, 063622 (2019).
36. C. M. Schmied, T. Gasenzer, P. B. Blakie, Violation of single-length-scaling dynamics via spin vortices in an isolated spin-1 Bose gas. *Phys. Rev. A (Coll. Park)* **100**, 033603 (2019).
37. R. Walz, K. Boguslavski, J. Berges, Large-N kinetic theory for highly occupied systems. *Phys. Rev. D* **97**, 116011 (2018).
38. I. Chantesana, A. Piñeiro Orioli, T. Gasenzer, Kinetic theory of nonthermal fixed points in a Bose gas. *Phys. Rev. A (Coll. Park)* **99**, 043620 (2019).
39. G. D. Moore, Condensates in relativistic scalar theories. *Phys. Rev. D* **93**, 065043 (2016).
40. J. Berges, B. Wallisch, Nonthermal fixed points in quantum field theory beyond the weak-coupling limit. *Phys. Rev. D* **95**, 036016 (2017).

41. J. Berges, K. Boguslavski, S. Schlichting, Nonlinear amplification of instabilities with longitudinal expansion. *Phys. Rev. D Part. Fields Gravit. Cosmol.* **85**, 076005 (2012).

42. J. Berges, K. Boguslavski, S. Schlichting, R. Venugopalan, Turbulent thermalization process in heavy-ion collisions at ultrarelativistic energies. *Phys. Rev. D Part. Fields Gravit. Cosmol.* **89**, 074011 (2014).

43. J. Berges, K. Boguslavski, S. Schlichting, R. Venugopalan, Universality far from equilibrium: From superfluid Bose gases to heavy-ion collisions. *Phys. Rev. Lett.* **114**, 061601 (2015).

44. K. Boguslavski, A. Kurkela, T. Lappi, J. Peuron, Highly occupied gauge theories in $2 + 1$ dimensions: A self-similar attractor. *Phys. Rev. D* **100**, 094022 (2019).

45. M. Prüfer *et al.*, Observation of universal dynamics in a spinor Bose gas far from equilibrium. *Nature* **563**, 217–220 (2018).

46. S. Erne, R. Bücker, T. Gasenzer, J. Berges, J. Schmiedmayer, Universal dynamics in an isolated one-dimensional Bose gas far from equilibrium. *Nature* **563**, 225–229 (2018).

47. C. Eigen *et al.*, Universal prethermal dynamics of Bose gases quenched to unitarity. *Nature* **563**, 221–224 (2018).

48. M. Prüfer *et al.*, Experimental extraction of the quantum effective action for a non-equilibrium many-body system. *Nat. Phys.* **16**, 1012–1016 (2020).

49. T. V. Zache, T. Schweigler, S. Erne, J. Schmiedmayer, J. Berges, Extracting the field theory description of a quantum many-body system from experimental data. *Phys. Rev. X* **10**, 011020 (2020).

50. J. A. P. Glidden *et al.*, Bidirectional dynamic scaling in an isolated Bose gas far from equilibrium. *Nat. Phys.* **17**, 457–461 (2021).

51. S. Smale *et al.*, Observation of a transition between dynamical phases in a quantum degenerate fermi gas. *Sci. Adv.* **5**, eaax1568 (2019).

52. J. Zhang *et al.*, Observation of a many-body dynamical phase transition with a 53-qubit quantum simulator. *Nature* **551**, 601–604 (2017).

53. A. Piñeiro Orioli *et al.*, Exploring dynamical phase transitions with cold atoms in an optical cavity. *Nature* **580**, 602–607 (2020).

54. A. Piñeiro Orioli, J. Berges, A. Piñeiro Orioli, J. Berges, Breaking the fluctuation-dissipation relation by universal transport processes. *Phys. Rev. Lett.* **122**, 150401 (2019).

55. K. Boguslavski, A. Piñeiro Orioli, Unraveling the nature of universal dynamics in $O(N)$ theories. *Phys. Rev. D* **101**, 091902 (2020).

56. S. Hild *et al.*, Far-from-equilibrium spin transport in Heisenberg quantum magnets. *Phys. Rev. Lett.* **113**, 147205 (2014).

57. P. N. Jepsen *et al.*, Spin transport in a tunable Heisenberg model realized with ultracold atoms. *Nature* **588**, 403–407 (2020).

58. P. N. Jepsen *et al.*, Transverse spin dynamics in the anisotropic Heisenberg model realized with ultracold atoms. *Phys. Rev. X* **11**, 041054 (2021).

59. S. Bhattacharyya, J. F. Rodriguez-Nieva, E. Demler, Universal prethermal dynamics in Heisenberg ferromagnets. *Phys. Rev. Lett.* **125**, 230601 (2020).

60. S. M. Davidson, A. Polkovnikov, SU(3) semiclassical representation of quantum dynamics of interacting spins. *Phys. Rev. Lett.* **114**, 045701 (2015).

61. J. Schachenmayer, A. Pikovski, A. M. Rey, Many-body quantum spin dynamics with Monte Carlo trajectories on a discrete phase space. *Phys. Rev. X* **5**, 011022 (2015).

62. J. F. Rodriguez-Nieva, Turbulent relaxation after a quench in the Heisenberg model. *Phys. Rev. B* **104**, L060302 (2021).

63. K. Boguslavski, A. Kurkela, T. Lappi, J. Peuron, Spectral function for overoccupied gluodynamics from real-time lattice simulations. *Phys. Rev. D* **98**, 014006 (2018).

64. A. Schachner, A. Piñeiro Orioli, J. Berges, Universal scaling of unequal-time correlation functions in ultracold Bose gases far from equilibrium. *Phys. Rev. A (Coll. Park)* **95**, 053605 (2017).

65. S. Schlichting, D. Smith, L. von Smekal, Spectral functions and critical dynamics of the O(4) model from classical-statistical lattice simulations. *Nucl. Phys. B* **950**, 114868 (2020).

66. A. Belavin, A. Polyakov, Metastable states of two-dimensional isotropic ferromagnets. *Sov. Phys. JETP* **22**, 503 (1975).

67. A. D. Rutenberg, W. J. Zakrzewski, M. Zapotocky, Dynamical multiscaling in quenched skyrme systems. *Europhys. Lett.* **39**, 49–54 (1997).

68. A. D. Rutenberg, A. J. Bray, Energy-scaling approach to phase-ordering growth laws. *Phys. Rev. E Stat. Phys. Plasmas Fluids Relat. Interdiscip. Topics* **51**, 5499–5514 (1995).

69. A. D. Rutenberg, Scaling violations with textures in two-dimensional phase ordering. *Phys. Rev. E Stat. Phys. Plasmas Fluids Relat. Interdiscip. Topics* **51**, R2715–R2718 (1995).

70. G. J. Stephens, Unraveling critical dynamics: The formation and evolution of textures. *Phys. Rev. D Part. Fields* **61**, 085002 (2000).

71. M. Babadi, E. Demler, M. Knap, Far-from-equilibrium field theory of many-body quantum spin systems: Prethermalization and relaxation of spin spiral states in three dimensions. *Phys. Rev. X* **5**, 041005 (2015).

72. J. F. Rodriguez-Nieva, A. Schuckert, D. Sels, M. Knap, E. Demler, Transverse instability and universal decay of spin spiral order in the Heisenberg model. *Phys. Rev. B* **105**, L060302 (2022).

73. J. F. Rodriguez-Nieva, D. Podolsky, E. Demler, Probing hydrodynamic sound modes in magnon fluids using spin magnetometers. *Phys. Rev. B* **105**, 174412 (2022).

74. S. Gopalakrishnan, R. Vasseur, Kinetic theory of spin diffusion and superdiffusion in *XXZ* spin chains. *Phys. Rev. Lett.* **122**, 127202 (2019).

75. S. Gopalakrishnan, D. A. Huse, V. Khemani, R. Vasseur, Hydrodynamics of operator spreading and quasiparticle diffusion in interacting integrable systems. *Phys. Rev. B* **98**, 220303 (2018).

76. A. J. Friedman, S. Gopalakrishnan, R. Vasseur, Diffusive hydrodynamics from integrability breaking. *Phys. Rev. B* **101**, 180302 (2020).

77. V. B. Bulchandani, R. Vasseur, C. Karrasch, J. E. Moore, Solvable hydrodynamics of quantum integrable systems. *Phys. Rev. Lett.* **119**, 220604 (2017).

78. V. B. Bulchandani, R. Vasseur, C. Karrasch, J. E. Moore, Bethe-Boltzmann hydrodynamics and spin transport in the XXZ chain. *Phys. Rev. B* **97**, 045407 (2018).

79. A. Polkovnikov, Phase space representation of quantum dynamics. *Ann. Phys.* **325**, 1790–1852 (2010).

80. C. Mora, Y. Castin, Extension of Bogoliubov theory to quasicondensates. *Phys. Rev. A* **67**, 053615 (2003).

81. B. Halperin, P. Hohenberg, Hydrodynamic theory of spin waves. *Phys. Rev.* **188**, 898 (1969).

82. A. Mazeliauskas, J. Berges, Prescaling and far-from-equilibrium hydrodynamics in the quark-gluon plasma. *Phys. Rev. Lett.* **122**, 122301 (2019).

83. C. M. Schmied, T. Gasenzer, Prescaling in a far-from-equilibrium Bose gas. *Phys. Rev. Lett.* **122**, 170404 (2019).

84. T. Dauxois, S. Ruffo, E. Arimondo, M. Wilkens, Eds., "Dynamics and thermodynamics of systems with long-range interactions: An introduction" in *Dynamics and Thermodynamics of Systems With Long-Range Interactions* (Springer, 2002), pp. 1–19.

85. A. V. Gorshkov *et al.*, Two-orbital SU(N) magnetism with ultracold alkaline-earth atoms. *Nat. Phys.* **6**, 289–295 (2010).

86. J. F. Rodriguez-Nieva, Data for "Far-from-equilibrium universality in the two-dimensional Heisenberg model." GitHub. Deposited 17 June 2022.